HHS Public Access

Author manuscript

J Cell Physiol. Author manuscript; available in PMC 2021 December 01.

Published in final edited form as:

J Cell Physiol. 2020 December ; 235(12): 9806–9818. doi:10.1002/jcp.29794.

Adjunctive mesenchymal stem/stromal cells augment microvascular function in post-stenotic kidneys treated with low-energy shockwave therapy

Xiao-Jun Chen[1,3], **Xin Zhang**[1], **Kai Jiang**[1], **James D. Krier**[1], **Xiangyang Zhu**[1], **Sabena Conley**[1], **Amir Lerman**[2], **Lilach O. Lerman**[1,2]

[1]Division of Nephrology and Hypertension, Mayo Clinic, Rochester, MN, United States

[2]Department of Cardiovascular Diseases, Mayo Clinic, Rochester, MN, United States

[3]Department of Nephrology, The Second Xiangya Hospital of Central South University, Changsha, Hunan, China.

Abstract

Effective therapeutic strategies are needed to preserve renal function in patients with atherosclerotic renal artery stenosis (ARAS). Low-energy shockwave therapy (SW) and adipose tissue-derived mesenchymal stem/stromal cells (MSCs) both stimulate angiogenesis repair of stenotic kidney injury. This study tested the hypothesis that intra-renal delivery of adipose tissue-derived MSCs would enhance the capability of SW to preserve stenotic kidney function and structure. Twenty-two pigs were studied after 16 weeks of ARAS, ARAS treated with a SW regimen (bi-weekly for 3 weeks) with or without subsequent intrarenal delivery of adipose tissue-derived MSCs, and controls. Four weeks after treatment, single-kidney renal blood flow (RBF) before and after infusion of acetylcholine, glomerular filtration rate (GFR), and oxygenation were assessed in vivo, and the renal microcirculation, fibrosis, and oxidative stress ex-vivo. Mean arterial pressure remained higher in ARAS, ARAS+SW, and ARAS+SW+MSC compared with Normal. Both SW and SW+MSC similarly elevated the decreased stenotic kidney GFR and RBF observed in ARAS to normal levels. Yet, SW+MSC significantly improved RBF response to acetylcholine in ARAS, and attenuated capillary loss and oxidative stress more than SW alone. Density of larger microvessels was similarly increased by both interventions. Therefore, while significant changes in functional outcome were not observed in the short-term, adjunct MSCs enhance pro-angiogenic effect of SW to improve renal microvascular outcomes, suggesting this as an effective strategy for long-term management of renovascular disease.

Correspondence: Lilach O. Lerman, MD, PhD, Division of Nephrology and Hypertension, Mayo Clinic, 200 First Street SW, Rochester, MN 55905. Fax: (507)-266-9316 Phone: (507)-266-9376 lerman.lilach@mayo.edu.

Authors' Contributions

X.J., A.L and L.O.L.designed the experiments. X.J.C.,X.J.,K.J., S.C, J.D.K. and X.Y.Z.acquired data. X.J.C. K.J.and J.D.K analyzed the data. X.J.C. and L.O.L. drafted the manuscript. All authors interpreted the results, revised the drafts, and approved the final version of the manuscript.

Data Availability Statement

The data that support the findings of this study are available from the corresponding author upon reasonable request.

Conflict of Interest Statement:

Dr. Lerman receives grant funding from Novo Nordisk, and is an advisor to Weijian Technologies and AstraZeneca.

Keywords

renal artery stenosis; extracorporeal shockwave; progenitor cells; renovascular endothelial function

Atherosclerotic renal artery stenosis (ARAS), the leading cause of renovascular hypertension, is increasingly encountered in the aging population(Hansen, Cherr, & Dean, 2002) and results in progressive renal functional loss and cardiovascular events (Lerman & Textor, 2001; Safian & Textor, 2001). Revascularization of the stenotic renal artery with percutaneous transluminal renal angioplasty (PTRA) slightly improves renovascular hypertension control compared to optimal medical treatment in human subjects with ARAS(Cooper et al., 2014), but recovery of renal function by PTRA and stenting is uncommon. This is likely because correction of an obstruction in the main renal artery alone cannot fully reverse downstream intrarenal damage distal to the stenosis (Eirin et al., 2011). Therefore, effective therapeutic strategies to directly attenuate renal tissue injury and promote its regeneration remain to be identified.

The stenotic kidney in ARAS is characterized by progressive renal functional deterioration secondary to microvascular remodeling, inflammation, fibrosis, and oxidative stress(Eirin, Textor, & Lerman, 2018), laying the foundation for employing novel therapeutic interventions, including pro-angiogenic, anti-inflammatory, anti-fibrotic, and antioxidant treatment. Our group has previously demonstrated that low-energy ultrasound extracorporeal shockwave (SW) therapy preserves post-stenotic kidney function in non-revascularized ARAS pigs, mainly by promoting ischemic kidney neovascularization, oxygenation, and perfusion(Zhang et al., 2016). However, the ability of SW to restore peritubular capillaries remains unclear.

Adipose tissue-derived mesenchymal stem/stromal cells (MSCs), a useful tool for cell-based therapy for preservation of the stenotic human kidney(Saad et al., 2017), secrete paracrine factors that activate repair program to preserve the renal capillary system(B. Ebrahimi et al., 2013; Eirin, Zhu, et al., 2018), decrease renal inflammation, and trigger tissue regeneration(Hickson, Eirin, & Lerman, 2016). Hence, addition of MSCs to a regimen of low-energy SW therapy may potentially enhance the ability of SW to repair the stenotic kidney in ARAS. This study was therefore designed to test the hypothesis that replenishment of MSC as an adjunct to SW would improve kidney outcomes compared to SW alone.

Materials and Methods

Animals and Experimental Design

Twenty-two domestic female pigs (50-60 Kg) were studied starting at 3 months of age for 16 weeks, after approval by the Institutional Animal Care and Use Committee. Pigs were randomized to Normal (n=6), untreated ARAS (n=6), ARAS treated with SW (n=5), or ARAS treated with MSC preceded by SW (n=5).

For the entire 16-week course of the study, normal pigs were fed normal pig chow (Figure 1), and ARAS pigs with a 2% high-cholesterol diet to promote early atherosclerosis.

Unilateral RAS was induced after 6 weeks of high-cholesterol diet by placing a local irritant coil in the right main renal artery, as previously described(Chade et al., 2002).

Autologous adipose tissue-derived MSCs were isolated using a standard protocol from porcine subcutaneous abdominal adipose tissue biopsy (5-10 g) collected three weeks after RAS induction(Conley et al., 2019; Eirin, Zhu, et al., 2018). Briefly, fat from each swine was harvested and minced and then digested in collagenase-H at 37°C for 45 min. After adding serum-containing medium, the suspension was filtered through a 100-μm cell strainer and centrifuged to pellet cells. Cells were further resuspended in advanced minimum essential medium supplemented with 5% platelet lysate (PLTmax, Mill Creek Life Sciences, Rochester, MN, USA), and expanded in culture for three passages for about 3 weeks. The 3rd passages of autologous MSCs was preserved in cell recovery medium in −80°C for transplantation. MSC were characterized by immunostaining and FlowSight (Amnis, Seattle, WA, USA) imaging flow cytometry (Figure 1) to determine cellular phenotype for the MSC markers CD90 and CD105, which was further confirmed by their trans-differentiation into osteocytes, chondrocytes and adipocytes (not shown), as previously described(Eirin et al., 2015). Cellular proliferation was determined over 72 hours with the live-cell analysis and imaging system Incucyte® (Satorius, Ann Arbor, MI)(Nargesi et al., 2019).

Then, starting 3 weeks after RAS induction, 10 ARAS pigs were treated twice a week for 3 weeks with sessions of low-energy SW. Guided by an Acuson SC2000 ultrasound system (Global Siemens Healthcare, Erlangen, Germany), SW was delivered through an ultrasound probe placed at the lateral aspect of the stenotic kidney, using Omnispec Vetspec Model (Medispec® LTD, Germantown, MD, USA; spark voltage 10-24 KV; energy density 0.09 mJ/mm^2; frequency 120 pulse/minute)(Zhang et al., 2016).

Six weeks after RAS induction, the degrees of stenosis in all the pigs were determined by renal angiography. Autologous adipose tissue-derived MSC were labeled with a fluorescent membrane dye (CellTrace™ Far Red), kept in 10ml PBS (10^6 cells/ml), and delivered into the stenotic kidney of 5 ARAS+SW pigs through a balloon placed in the renal artery proximal to the stenosis(Zhu et al., 2013). A vehicle (saline) was administered in the 5 other ARAS+SW pigs. Four weeks after delivery of MSC or sham, renal function and oxygenation were assessed using multi-detector computed tomography (MDCT) and blood oxygen-level dependent (BOLD) magnetic resonance imaging (MRI), respectively, 2-3 days apart. Animals were euthanized three days after in vivo studies with a lethal intravenous dose of sodium pentobarbital (100 mg/kg). The kidneys were removed, and sections frozen in liquid nitrogen, or preserved in formalin for histology.

In Vivo Studies

Blood Pressure and Renal Function—Single-kidney renal blood flow (RBF) and glomerular filtration rate (GFR) were assessed using MDCT, as described previously (Chade et al., 2002; Daghini et al., 2007). For this purpose, 160 consecutive kidneys scans were performed following a central venous bolus injection of iopamidol ($0.5\ ml{\cdot}kg^{-1}{\cdot}2s^{-1}$), and repeated during suprarenal infusion of the endothelium-dependent vasodilator acetylcholine (ACh, 5μm/kg/min), to test intrarenal microvascular endothelial function. Then, MDCT images were reconstructed and displayed with the Analyze® software package (Biomedical

Imaging Resource, Mayo Clinic, Rochester, MN). For data analysis, the aorta, renal cortex, and medulla were all traced on tomographic images to produce time-attenuation curves in each region, which were fitted by curve-fitting algorithms, and estimates of renal function were obtained. Renal volume was determined from a separate scan.

Renal Oxygenation—BOLD-MRI (3T Signa Echo Speed; GE Medical Systems, Milwaukee, WI) scanning was performed under isoflurane (1-2%) anesthesia to assess intra-renal oxygenation (evaluated as R2*) (L. Warner et al., 2011; L. Warner et al., 2009) . Sixteen T_2*-weighted images were acquired with echo times from 2.1 to 27 ms. For data analysis, MR images in cortex and medulla acquired with increasing echo times were used to calculate their regression with the signal logarithm, with a slope (R2*=1/T2*) related to deoxyhemoglobin levels and thence blood and tissue oxygen content.

Ex vivo studies

Four weeks after delivery, labeled MSC were tracked in frozen stenotic-kidney sections stained with nuclear 4′,6-diamidino-2-phenylindole (DAPI). Stenotic-kidney MSC retention rate (percentage of injected cells detected in the organ) was calculated as previously described(Eirin et al., 2015).

To assess the renal microvasculature (microvessels with diameters 40-500μm), the stenotic kidney was flushed and perfused with microfil MV122 (an intravascular contrast agent) through a cannula ligated in the renal artery. Images were acquired from scanning at 0.5° angular increments at 18-μm resolution, and analyzed as previously described(Zhang et al., 2016). The spatial density of microvessels in the inner and outer renal cortex was calculated.

Renal peritubular capillaries were identified in 5μm slides stained by H&E by the presence of lumen, red blood cells, and/or an endothelial cell lining. Capillaries were counted at 100× magnification using an ApoTome microscope (Carl ZEISS SMT, Oberkochen, Germany), and the ratio of capillary number to tubules calculated(Eirin, Zhu, et al., 2018). In addition, endothelial cells density was assessed by area of von Willebrand factor (vWF) (1:200 Abcam) immunoreactivity by immunofluorescent staining. Fibrosis was evaluated by Masson trichrome staining and quantified semi-automatically as percent area staining (using AxioVision 4.8, ZEISS).

Oxidative stress was evaluated ex-vivo by the in-situ production of superoxide anion (dihydroethidium, DHE)(Chade et al., 2004), and immunofluorescent staining for 8-hydroxy-2’ -deoxyguanosine (8-OHdG) (1:500 Abcam) and oxidized low-density lipoprotein (Ox-LDL) (1:100 Millipore). 8-OHDG+ and total nuclei were manually counted on 10 fields (40x), and their ratio calculated. Ox-LDL immunoreactivity was assessed as percent area.

Renal expression of endothelial nitric oxide synthase (eNOS) and monocyte chemoattractant protein (MCP)-1 was evaluated by western blotting(Eirin, Ebrahimi, et al., 2014). For inflammatory markers, blood samples were collected from the renal vein (RV) as previously described(Eirin, Zhang, et al., 2014), and plasma levels of tumor necrosis factor (TNF)-α,

interferon (IF)-γ, and interleukin (IL)-10 were measured by enzyme-linked immunosorbent assay (R&D PTA00, Kingfisher VS0259S-002, and R&D P1000).

Statistical methods

Statistical analysis was performed using JMP software package version 14.0 (SAS Institute. Cary, NC). Results were expressed as mean±SEM for normally distributed variables. Comparisons within groups were performed using the paired Student t-test, and among groups using parametric (ANOVA and unpaired t-test with Bonferroni correction) and nonparametric (Wilcoxon/Kruskal-Wallis) tests as appropriate. Statistical significance for all tests was accepted for $p<0.05$.

Results

Six weeks after stenosis induction, the degree of stenosis in the ARAS, ARAS+SW, and ARAS+SW+MSC groups was comparable (p=0.78, ANOVA Table 1).

MSCs characterization and engraftment in the stenotic kidney

MSC studied by flow cytometry showed purity of ≥98% and positivity for the typical MSC markers CD105 and CD90, and showed avid capacity for proliferation *in vitro* (Figure 1B). Their retention rate in the stenotic kidney 4 weeks after intra-arterial administration (Figure 1C) was 6.8±2.4%.

SW and SW+MSC do not lower BP

At 16 weeks, plasma renin activity (PRA) was elevated in the ARAS stenotic kidney veins, but decreased by SW and SW+MSC, indicating decreased activation of the renin-angiotensin system. SW and SW+MSC tended to, but neither one significantly lowered MAP in ARAS (Table 1).

Both treatments restored renal function

MDCT-derived RBF and GFR of the stenotic ARAS kidney decreased compared to normal (Figure 2A-B, p=0.007 and p=0.004, respectively), indicating a hemodynamically significant stenosis. Both SW and SW+MSC improved RBF (p=0.02 and p=0.04 vs. ARAS) and normalized GFR (p=0.3 and p=0.1 vs. Normal, respectively), indicating that both treatments restored stenotic kidney hemodynamics and function. There was no difference among the groups in contralateral kidney GFR (p=0.09 ANOVA).

Only SW+MSC improved endothelial function

RBF responses to Ach were used as an index of renal microvascular endothelial function. Ach significantly increased RBF in all the groups. However, in ARAS and ARAS+SW the degree of RBF responses to Ach was blunted (Figure 2C, p=0.003 and p=0.03 vs. Normal, respectively), yet was normalized in ARAS+SW+MSC (p=0.45 vs. Normal). Therefore, addition of MSC in ARAS+SW+MSC pigs successfully alleviated microvascular endothelial dysfunction in the stenotic kidney.

SW and SW+MSC attenuated renal hypoxia

BOLD-MRI was used to assess renal oxygenation (and reciprocally R2*, the index of hypoxia). Renal cortical and medullary hypoxia (R_2*) was elevated in ARAS (Figure 2D-E, p=0.003 and p<0.001 vs. Normal, respectively), but restored to normal oxygenation levels in ARAS+SW and ARAS+SW+MSC in both the cortex (p=0.03 and p=0.04 vs. ARAS, p=0.2 and p=0.1 vs. Normal, respectively) and medulla (p<0.001 and p=0.006 vs. ARAS, p=0.3 and p=0.2 vs. Normal, respectively). These observations suggest that the two treatment modalities had a comparable effect to blunt renal hypoxia.

The microcirculation was improved in SW-MSC-treated swine

Cortical microvessels and peritubular capillaries were evaluated to assess the ability of SW and SW+MSC to avert loss of different-size vessels in the stenotic kidney. ARAS decreased the density of cortical microvessels (Figure 2D, F, p<0.01 vs. Normal), but this was normalized by both SW (p=0.9 vs. Normal, p=0.009 vs. ARAS) and SW+MSC (p=0.9 vs. Normal, p=0.03 vs. ARAS).

Similarly, cortical and medullary capillary density assessed in H&E-stained slides was significantly lower in ARAS compared to normal kidneys (p<0.001), but significantly higher in both ARAS+SW and ARAS+SW+MSC (Figure 3A-B, p=0.003 and p<0.001 vs. ARAS, respectively), and in the cortex was not different from Normal (both p=0.01). Yet, the number of cortical capillaries was higher in ARAS+SW+MSC than in ARAS+SW (p=0.007). Medullary capillary density improved (p=0.04 and p=0.02 vs. ARAS, respectively), but remained blunted in both treatment groups (p<0.001 and p=0.001 vs. Normal, respectively). Immunoreactivity of vWF, a marker of endothelial cells, was also diminished compared to Normal in the ARAS cortex and medulla (p=0.006 and p=0.009, respectively), was restored in ARAS+SW+MSC (p=0.2 and p=0.5 vs. Normal, respectively), but remained blunted in ARAS+SW (p=0.003 and p=0.02 vs. Normal, respectively, Supplement Figure 1), possibly because vWF detects also microvessels larger than capillaries. Hence, SW+MSC was more effective than SW alone to restore the microcirculation.

SW+MSC reduced oxidative stress and up-regulated eNOS expression

To explore mechanisms associated with microvascular endothelial dysfunction in stenotic kidneys, eNOS expression was used to assess bioavailability of the vasodilator nitric oxide, whereas *in-situ* production of superoxide anion (which quenches nitric oxide) by DHE staining, and expression of 8-OHdG and Ox-LDL by immunofluorescence staining, were used to evaluate oxidative stress. DHE staining revealed increased oxidative stress in the ARAS kidney (Figure 4A-B, p=0.009 vs. Normal), which was not different from ARAS in ARAS+SW, but was abolished by SW+MSC (p=0.01 vs. untreated ARAS). In addition, expression of 8-OHdG, a biomarker of oxidative DNA damage, markedly increased in ARAS (Figure 4A-B, p<0.001 vs. Normal), decreased by SW (p=0.003 vs. ARAS) and further decreased by SW+MSC (p=0.02 vs. ARAS+SW). SW and SW+MSC (Figure 4A-B, p=0.03 and p=0.01 vs. ARAS respectively) similarly decreased Ox-LDL expression upregulated in ARAS (p<0.001 vs. Normal). The expression of eNOS remained unchanged in ARAS and ARAS+SW groups (Figure 5A-B, Supplement Figure 2, p=0.2 and p=0.3 vs.

Normal, respectively), but was markedly upregulated by SW+MSC compared to all other groups (p=0.004 vs. Normal, p=0.01 vs. ARAS, p=0.003 vs. ARAS+SW). Therefore, SW +MSC more effectively reduced oxidative stress and up-regulated eNOS expression, which might have accounted for improved microvascular endothelial function.

SW and SW+MSC attenuated kidney inflammation

Renal protein expression of the inflammatory mediator MCP-1 significantly increased in ARAS compared to Normal (Figure 5A-B, Supplement Figure 2, p=0.03). It was blunted and tended to be lower than normal in both SW and SW+MSC (p=0.06 and p=0.08 vs. Normal, respectively), with no significant difference between the groups. Similarly, RV TNF-a level significantly increased almost fourfold in ARAS vs. Normal (Table 1, p=0.01), and both SW and SW+MSC tended to decrease it (both p=0.1 vs ARAS). RV IL-10 level was unchanged in ARAS, but tended to increase by SW (p=0.1 vs ARAS and Normal), and was further significantly increased by SW+MSC (p=0.03 vs ARAS and p=0.02 vs Normal). RV levels of IF-γ were similar among the groups. Therefore, SW tends to decrease pro-inflammatory mediators, while adjunctive MSC therapy boosts anti-inflammatory (IL-10) mediators.

Similar beneficial effect of SW and SW+MSC on kidney fibrosis

Marked medullary and cortical fibrosis (by trichrome-staining) was observed in ARAS kidneys (Figure 5C-D, both p<0.001 vs. Normal). Fibrosis was attenuated in both SW and SW+MSC compared to ARAS (p=0.002 and p=0.006 in cortex, p=0.02 and p=0.01 in medulla, respectively), although both remained higher than Normal (both p<0.001 in cortex, p=0.01 and p=0.05 in medulla, respectively) with no significant difference between the two. Therefore, SW and SW+MSC had comparable effects on kidney fibrosis.

Discussion

The present study demonstrates that low-energy SW improves GFR and RBF and ameliorates fibrosis, hypoxia, and inflammation in the post-stenotic kidney. However, addition of MSC increases the number of peritubular capillaries and restores microvascular endothelial function, indicated by greater RBF response to Ach, possibly by increasing nitric oxide bioavailability, decreasing renal oxidative stress, and upregulating anti-inflammatory mediators. These observations indicated that adjunct delivery of MSC might augment the effects of SW therapy on preservation of microvascular function in the stenotic kidney.

The mechanisms responsible for renal damage in ARAS include hemodynamic aberrations, renal tissue inflammation, hypoxia, oxidative stress, and microvascular remodeling, which lead to renal scarring(Eirin, Textor, et al., 2018). Strategies targeting these mechanisms to attenuate kidney injury may slow down progression of chronic kidney disease, or might enhance potential benefits secondary to restoration of renal flow(X. J. Chen et al., 2019). Of note, both SW and SW+MSC treatments were capable of attenuating damage in the stenotic kidney without affecting blood pressure, likely targeting directly injurious mechanisms in ARAS. In congruence, swine and murine studies showed that antioxidant, anti-fibrosis, or MSC-derived extracellular vesicles strategies can all improve renal function, despite

unchanged renovascular hypertension (Chade et al., 2004; Eirin et al., 2017; G. M. Warner et al., 2012). Based on our previously studies, SW may reverse renal dysfunction by up-regulation of angiogenic factor expression through mechanotransduction, resulting in restoration of the renal microcirculation(Zhang et al., 2016). We have also shown that MSCs improve remodeling and reduce oxidative stress and inflammation in the stenotic kidney via paracrine mechanisms(Eirin et al., 2012b; Zhu et al., 2013). Therefore, we hypothesized that concurrent delivery of MSCs and SW would improve renal microvascular outcomes in the stenotic kidneys.

Indeed, we observed that SW+MSC improved RBF response to Ach (reflecting improved endothelial function), possibly by up-regulating levels of eNOS and reducing oxidative stress. eNOS exerts a vasculoprotective effect primarily by eliciting release of nitric oxide, and partly by counterbalancing the effects of the renin-angiotensin system(Forbes, Thornhill, Park, & Chevalier, 2007). MSCs up-regulate eNOS expression in endothelial cells by mediating IL-8/macrophage inflammatory protein-2(Lin, Yet, Hsu, Wang, & Hung, 2015). Increased oxidative stress in the stenotic kidney might be secondary to hypoxia associated with renal microvascular remodeling(Zhu et al., 2004) and inefficient oxygen handling. We found that addition of MSCs to SW decreased DHE and 8-OHDG staining in ARAS, indicating reduced superoxide production and DNA damage, although lipid oxidation (ox-LDL) was attenuated by SW regardless of MSC addition. In agreement, MSCs were shown to suppress oxidative stress in experimental renal artery stenosis(Zhu et al., 2013), kidney ischemia-reperfusion injury(Y. T. Chen et al., 2011) and diabetic nephropathy(Lv et al., 2014). Since endothelial dysfunction has deleterious effects on renal function(Perticone et al., 2010), the ability of SW+MSC to effectively restore renovascular endothelial function may in turn maintain microvascular integrity(Bonetti, Lerman, & Lerman, 2003; O'Riordan et al., 2005) and prevent long-term renal worsening.

Loss of microvascular integrity plays a central role in progression of renal damage in ARAS(Eirin, Textor, et al., 2018). We have shown that both SW(Zhang et al., 2016) and MSCs(B. Ebrahimi et al., 2013; Eirin, Zhu, et al., 2018) could preserve the renal microvasculature and promote proliferation of small-to-large microvessels (40-500μm in diameter), the former through mechanotransduction and the latter possibly via paracrine effects. In the present study, intra-arterial delivery of MSCs to SW resulted in superior preservation of vWF staining and capillary density, an important correlate of renal disease progression(Venkatachalam & Weinberg, 2017). Therefore, this combination may further attenuate post-stenotic renal damage and improve renal recovery. Notably, the medulla demonstrated blunted vascular repair compared with the cortex. We have previously observed that fewer MSCs reached the stenotic kidney medulla compared to the cortex (cortical-medullary engraftment ratio=5:1), and following PTRA facilitated improvement in RBF, but not in medullary flow(Behzad Ebrahimi et al., 2013; Eirin et al., 2012a). Similarly, the SW beam may penetrate the deep medulla less effectively than the cortex, and thus both treatments were less effective in medullary vascular repair.

Interestingly, we found that SW+MSC exerted greater efficacy in increasing the anti-inflammatory factor IL-10, which mediates the paracrine actions of MSC to preserve kidneys subjected to chronic ischemia (Eirin et al., 2017). These observations suggest a

greater anti-inflammatory potency of adjunctive MSC, blunting capillary rarefaction(Afsar et al., 2018).

In contrast to the cortical microcirculation, addition MSCs to SW did not augment the improvement of RBF or renal function. Possibly, the effects of enhanced endothelial function and capillary density on stenotic-kidney RBF is long-term and was not captured within our observation period. Alternatively, autologous adipose tissue-derived MSC isolated from ARAS subjects might have had imperfect function(Saad et al., 2016). For example, the saturated fatty-acid palmitate may induce apoptosis in human bone marrow-derived MSCs and decrease their proliferation(Fillmore et al., 2015), and hyperlipidemia may compromise their homing efficiency(Xu et al., 2014). Indeed, we have shown that MSC from patients with ARAS had increased DNA damage and reduced pro-angiogenic function(Saad et al., 2016). However, for practical purposes and potential clinical application, it is relevant to study the effects of autologous MSCs, which are safer and less susceptible to rejection, even if not entirely normal. MSCs also did not boost BP improvement compared to SW alone, in line with our previous study showing no effect of MSC on renovascular hypertension(Zhu et al., 2011). Probably due to the persisting obstruction in the renal artery, PRA decreased but was not normalizes by either treatment, which might have contributed to sustained hypertension.

There are obvious limitations for replicating clinical conditions by the short duration of ARAS, as the model was developed over 16 weeks with short-term exposures to atherosclerosis and renovascular disease. Nevertheless, disease development and renal pathology in our porcine model closely resemble the human condition. Notably, in the present study, we found in the stenotic kidney a lower MSCs retention rate than that of allogeneic MSCs isolated from normal swine (6.8±2.4% vs. 13.1±2.2%)(Eirin et al., 2012a). Hence, higher doses or repeated deliveries might be required to achieve greater therapeutic benefits of autologous cells from subjects with ARAS. Furthermore, longer-term benefits of treatment remain to be determined. Additional studies are also needed to determine the optimal SW or cell delivery regimen.

Conclusion

The current study shows that addition of MSCs improves density of capillaries (but not necessarily larger microvessels) and microvascular endothelial function in vivo in SW-treated stenotic kidneys, probably by attenuating oxidative stress and inflammation. While in the short-term this may not translate to enhanced renal function, this strategy might be effective for long-term management of renovascular disease. Additional strategies are needed to improve blood pressure control, and possibly explore the combination of SW with additional therapeutic strategies.

Supplementary Material

Refer to Web version on PubMed Central for supplementary material.

Acknowledgment

We thank Medispec® LTD, Gaithersburg, MD, for generously allowing the use of the SW machine. The vendor was not involved in data collection or analysis.

Sources of Funding

This research was partly supported by NIH grants numbers HL123160, DK104273, DK102325, DK120292, DK122734, and the American Heart Association.

References

Afsar B, Afsar RE, Dagel T, Kaya E, Erus S, Ortiz A, . . . Kanbay M (2018). Capillary rarefaction from the kidney point of view. Clin Kidney J, 11(3), 295–301. doi:10.1093/ckj/sfx133 [PubMed: 29988260]

Bonetti PO, Lerman LO, & Lerman A (2003). Endothelial Dysfunction: A Marker of Atherosclerotic Risk. Arterioscler Thromb Vasc Biol, 23(2), 168–175. [PubMed: 12588755]

Chade AR, Krier JD, Rodriguez-Porcel M, Breen JF, McKusick MA, Lerman A, & Lerman LO (2004). Comparison of acute and chronic antioxidant interventions in experimental renovascular disease. Am J Physiol Renal Physiol, 286(6), F1079–1086. doi:10.1152/ajprenal.00385.2003 [PubMed: 14722019]

Chade AR, Rodriguez-Porcel M, Grande JP, Krier JD, Lerman A, Romero JC, . . . Lerman LO (2002). Distinct renal injury in early atherosclerosis and renovascular disease. Circulation, 106(9), 1165–1171. [PubMed: 12196346]

Chen XJ, Zhang X, Jiang K, Krier JD, Zhu XY, Lerman A, & Lerman LO (2019). Improved renal outcomes after revascularization of the stenotic renal artery in pigs by prior treatment with low-energy extracorporeal shockwave therapy. J Hypertens, 37(in press).

Chen YT, Sun CK, Lin YC, Chang LT, Chen YL, Tsai TH, . . . Yip HK (2011). Adipose-derived mesenchymal stem cell protects kidneys against ischemia-reperfusion injury through suppressing oxidative stress and inflammatory reaction. J Transl Med, 9, 51. doi:10.1186/1479-5876-9-51 [PubMed: 21545725]

Conley SM, Shook JE, Zhu XY, Eirin A, Jordan KL, Woollard JR, . . . Lerman LO (2019). Metabolic Syndrome Induces Release of Smaller Extracellular Vesicles from Porcine Mesenchymal Stem Cells. Cell Transplant, 28(9–10), 1271–1278. doi:10.1177/0963689719860840 [PubMed: 31250656]

Cooper CJ, Murphy TP, Cutlip DE, Jamerson K, Henrich W, Reid DM, . . . Investigators, C. (2014). Stenting and medical therapy for atherosclerotic renal-artery stenosis. N Engl J Med, 370(1), 13–22. doi:10.1056/NEJMoa1310753 [PubMed: 24245566]

Daghini E, Primak AN, Chade AR, Krier JD, Zhu XY, Ritman EL, . . . Lerman LO (2007). Assessment of renal hemodynamics and function in pigs with 64-section multidetector CT: comparison with electron-beam CT. Radiology, 243(2), 405–412. [PubMed: 17456868]

Ebrahimi B, Eirin A, Li Z, Zhu X-Y, Zhang X, Lerman A, . . . Lerman LO (2013). Mesenchymal Stem Cells Improve Medullary Inflammation and Fibrosis after Revascularization of Swine Atherosclerotic Renal Artery Stenosis. PLoS One, 8(7), e67474 67471–67412. doi:10.1371/journal.pone.0067474 [PubMed: 23844014]

Ebrahimi B, Eirin A, Li Z, Zhu XY, Zhang X, Lerman A, . . . Lerman LO (2013). Mesenchymal stem cells improve medullary inflammation and fibrosis after revascularization of swine atherosclerotic renal artery stenosis. PLoS One, 8(7), e67474. doi:10.1371/journal.pone.0067474 [PubMed: 23844014]

Eirin A, Ebrahimi B, Zhang X, Zhu XY, Woollard JR, He Q, . . . Lerman LO (2014). Mitochondrial protection restores renal function in swine atherosclerotic renovascular disease. Cardiovasc Res, 103(4), 461–472. doi:10.1093/cvr/cvu157 [PubMed: 24947415]

Eirin A, Textor SC, & Lerman LO (2018). Emerging Paradigms in Chronic Kidney Ischemia. Hypertension, 72(5), 1023–1030. doi:10.1161/HYPERTENSIONAHA.118.11082 [PubMed: 30354824]

Eirin A, Zhang X, Zhu XY, Tang H, Jordan KL, Grande JP, . . . Lerman LO (2014). Renal vein cytokine release as an index of renal parenchymal inflammation in chronic experimental renal artery stenosis. Nephrol Dial Transplant, 29(2), 274–282. doi:10.1093/ndt/gft305 [PubMed: 24097799]

Eirin A, Zhu XY, Ferguson CM, Riester SM, van Wijnen AJ, Lerman A, & Lerman LO (2015). Intra-renal delivery of mesenchymal stem cells attenuates myocardial injury after reversal of hypertension in porcine renovascular disease. Stem Cell Res Ther, 6, 7. doi:10.1186/scrt541 [PubMed: 25599803]

Eirin A, Zhu XY, Jonnada S, Lerman A, van Wijnen AJ, & Lerman LO (2018). Mesenchymal Stem Cell-Derived Extracellular Vesicles Improve the Renal Microvasculature in Metabolic Renovascular Disease in Swine. Cell Transplant, 27(7), 1080–1095. doi:10.1177/0963689718780942 [PubMed: 29954220]

Eirin A, Zhu XY, Krier JD, Tang H, Jordan KL, Grande JP, . . . Lerman LO (2012a). Adipose tissue-derived mesenchymal stem cells improve revascularization outcomes to restore renal function in swine atherosclerotic renal artery stenosis. Stem Cells, 30(5), 1030–1041. doi:10.1002/stem.1047 [PubMed: 22290832]

Eirin A, Zhu XY, Krier JD, Tang H, Jordan KL, Grande JP, . . . Lerman LO (2012b). Adipose tissue-derived mesenchymal stem cells improve revascularization outcomes to restore renal function in swine atherosclerotic renal artery stenosis. Stem Cells, 30(5), 1030–1041. doi:10.1002/stem.1047 [PubMed: 22290832]

Eirin A, Zhu XY, Puranik AS, Tang H, McGurren KA, van Wijnen AJ, . . . Lerman LO (2017). Mesenchymal stem cell-derived extracellular vesicles attenuate kidney inflammation. Kidney Int, 92(1), 114–124. doi:10.1016/j.kint.2016.12.023 [PubMed: 28242034]

Eirin A, Zhu XY, Urbieta-Caceres VH, Grande JP, Lerman A, Textor SC, & Lerman LO (2011). Persistent kidney dysfunction in swine renal artery stenosis correlates with outer cortical microvascular remodeling. Am J Physiol Renal Physiol, 300(6), F1394–1401. doi:10.1152/ajprenal.00697.2010 [PubMed: 21367913]

Fillmore N, Huqi A, Jaswal JS, Mori J, Paulin R, Haromy A, . . . Lopaschuk GD (2015). Effect of fatty acids on human bone marrow mesenchymal stem cell energy metabolism and survival. PLoS One, 10(3), e0120257. doi:10.1371/journal.pone.0120257 [PubMed: 25768019]

Forbes MS, Thornhill BA, Park MH, & Chevalier RL (2007). Lack of endothelial nitric-oxide synthase leads to progressive focal renal injury. Am J Pathol, 170(1), 87–99. doi:10.2353/ajpath.2007.060610 [PubMed: 17200185]

Hansen KJ, Cherr GS, & Dean RH (2002). Dialysis-free survival after surgical repair of ischemic nephropathy. Cardiovasc Surg, 10(4), 400–404. [PubMed: 12359416]

Hickson LJ, Eirin A, & Lerman LO (2016). Challenges and opportunities for stem cell therapy in patients with chronic kidney disease. Kidney Int, 89(4), 767–778. doi:10.1016/j.kint.2015.11.023 [PubMed: 26924058]

Lerman L, & Textor SC (2001). Pathophysiology of ischemic nephropathy. Urol Clin North Am, 28(4), 793–803, ix. [PubMed: 11791495]

Lin YL, Yet SF, Hsu YT, Wang GJ, & Hung SC (2015). Mesenchymal Stem Cells Ameliorate Atherosclerotic Lesions via Restoring Endothelial Function. Stem Cells Transl Med, 4(1), 44–55. doi:10.5966/sctm.2014-0091 [PubMed: 25504897]

Lv S, Cheng J, Sun A, Li J, Wang W, Guan G, . . . Su M (2014). Mesenchymal stem cells transplantation ameliorates glomerular injury in streptozotocin-induced diabetic nephropathy in rats via inhibiting oxidative stress. Diabetes Res Clin Pract, 104(1), 143–154. doi:10.1016/j.diabres.2014.01.011 [PubMed: 24513119]

Nargesi AA, Zhu XY, Conley SM, Woollard JR, Saadiq IM, Lerman LO, & Eirin A (2019). Renovascular disease induces mitochondrial damage in swine scattered tubular cells. Am J Physiol Renal Physiol, 317(5), F1142–F1153. doi:10.1152/ajprenal.00276.2019 [PubMed: 31461348]

O'Riordan E, Chen J, Brodsky SV, Smirnova I, Li H, & Goligorsky MS (2005). Endothelial cell dysfunction: The syndrome in making. Kidney Int, 67(5), 1654–1658. [PubMed: 15840005]

Perticone F, Maio R, Perticone M, Sciacqua A, Shehaj E, Naccarato P, & Sesti G (2010). Endothelial dysfunction and subsequent decline in glomerular filtration rate in hypertensive patients.

Circulation, 122(4), 379–384. doi:10.1161/CIRCULATIONAHA.110.940932 [PubMed: 20625109]

Saad A, Dietz AB, Herrmann SMS, Hickson LJ, Glockner JF, McKusick MA, . . . Textor SC (2017). Autologous Mesenchymal Stem Cells Increase Cortical Perfusion in Renovascular Disease. J Am Soc Nephrol, 28(9), 2777–2785. doi:10.1681/ASN.2017020151 [PubMed: 28461553]

Saad A, Zhu XY, Herrmann S, Hickson L, Tang H, Dietz AB, . . . Textor S (2016). Adipose-derived mesenchymal stem cells from patients with atherosclerotic renovascular disease have increased DNA damage and reduced angiogenesis that can be modified by hypoxia. Stem Cell Res Ther, 7(1), 128. doi:10.1186/s13287-016-0389-x [PubMed: 27612459]

Safian RD, & Textor SC (2001). Renal-artery stenosis. N Engl J Med, 344(6), 431–442. doi:10.1056/NEJM200102083440607 [PubMed: 11172181]

Venkatachalam MA, & Weinberg JM (2017). Pericytes Preserve Capillary Integrity to Prevent Kidney Hypoxia. J Am Soc Nephrol, 28(3), 717–719. doi:10.1681/ASN.2016111157 [PubMed: 27979991]

Warner GM, Cheng J, Knudsen BE, Gray CE, Deibel A, Juskewitch JE, . . . Grande JP (2012). Genetic deficiency of Smad3 protects the kidneys from atrophy and interstitial fibrosis in 2K1C hypertension. Am J Physiol Renal Physiol, 302(11), F1455–1464. doi:10.1152/ajprenal.00645.2011 [PubMed: 22378822]

Warner L, Glockner JF, Woollard J, Textor SC, Romero JC, & Lerman LO (2011). Determinations of renal cortical and medullary oxygenation using blood oxygen level-dependent magnetic resonance imaging and selective diuretics. Invest Radiol, 46(1), 41–47. [PubMed: 20856128]

Warner L, Gomez SI, Bolterman R, Haas JA, Bentley MD, Lerman LO, & Romero JC (2009). Regional decreases in renal oxygenation during graded acute renal arterial stenosis: a case for renal ischemia. Am J Physiol Regul Integr Comp Physiol, 296(1), R67–71. doi:10.1152/ajpregu.90677.2008 [PubMed: 18971350]

Xu QC, Hao PJ, Yu XB, Chen SL, Yu MJ, Zhang J, & Yang PS (2014). Hyperlipidemia compromises homing efficiency of systemically transplanted BMSCs and inhibits bone regeneration. Int J Clin Exp Pathol, 7(4), 1580–1587. [PubMed: 24817954]

Zhang X, Krier JD, Amador Carrascal C, Greenleaf JF, Ebrahimi B, Hedayat AF, . . . Lerman LO (2016). Low-Energy Shockwave Therapy Improves Ischemic Kidney Microcirculation. J Am Soc Nephrol, 27(12), 3715–3724. doi:10.1681/ASN.2015060704 [PubMed: 27297945]

Zhu XY, Chade AR, Rodriguez-Porcel M, Bentley MD, Ritman EL, Lerman A, & Lerman LO (2004). Cortical microvascular remodeling in the stenotic kidney: role of increased oxidative stress. Arterioscler Thromb Vasc Biol, 24(10), 1854–1859. doi:10.1161/01.ATV.0000142443.52606.81 [PubMed: 15308558]

Zhu XY, Urbieta Caceres VH, Favreau FD, Krier JD, Lerman A, & Lerman LO (2011). Enhanced endothelial progenitor cell angiogenic potency, present in early experimental renovascular hypertension, deteriorates with disease duration. J Hypertens, 29(10), 1972–1979. doi:10.1097/HJH.0b013e32834ae611 [PubMed: 21873884]

Zhu XY, Urbieta-Caceres V, Krier JD, Textor SC, Lerman A, & Lerman LO (2013). Mesenchymal stem cells and endothelial progenitor cells decrease renal injury in experimental swine renal artery stenosis through different mechanisms. Stem Cells, 31(1), 117–125. doi:10.1002/stem.126 [PubMed: 23097349]

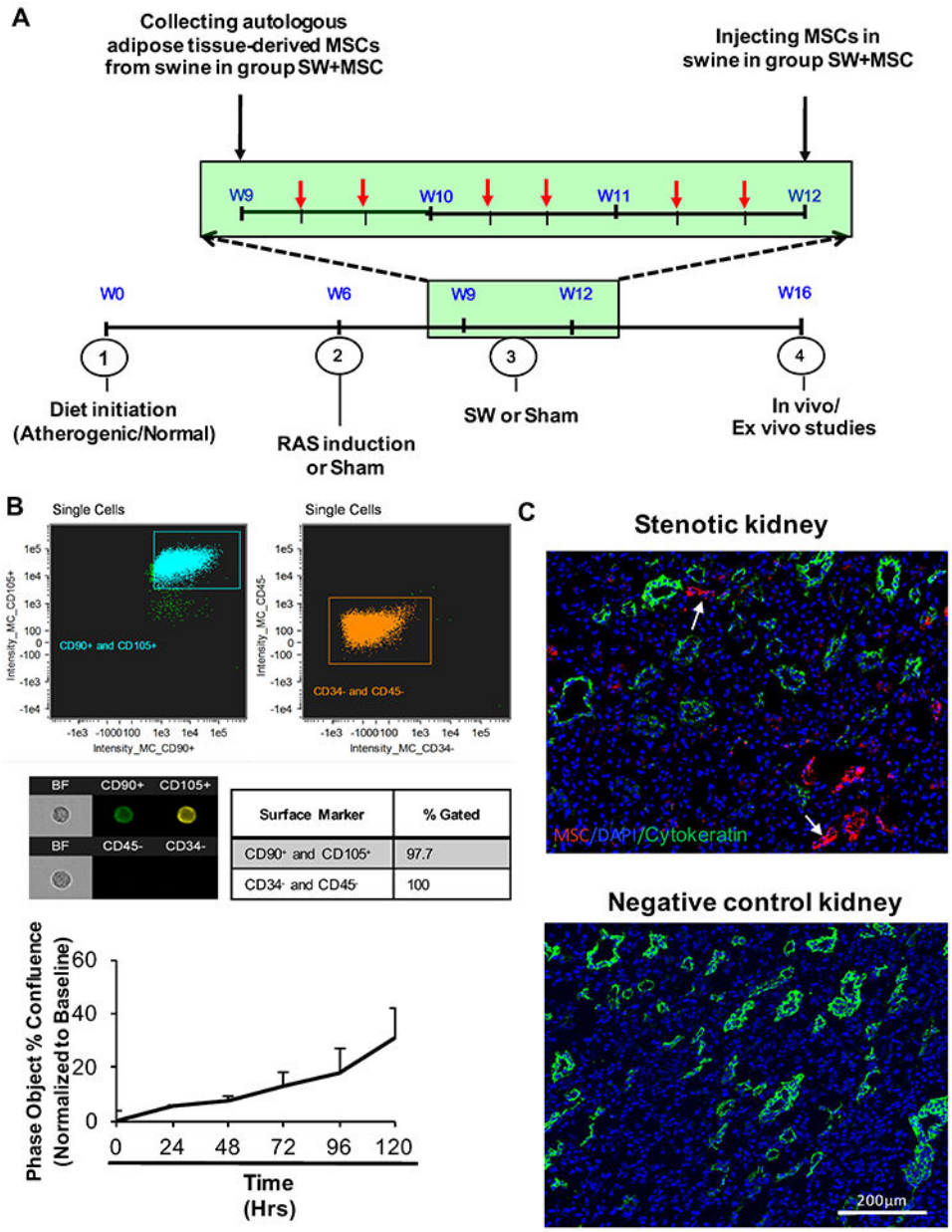

Figure 1.

A. Schematic of a 16-wk experimental protocol, with 6 shockwave (SW) therapy sessions delivered over a 3-week regimen (weeks 9, 10, and 11; each session indicated by a red arrow), and autologous adipose tissue-derived mesenchymal stem/stromal cells (MSCs) collection at the beginning of week 9 and injection at the end of week 11 (black arrow). **B.** Characterization of MSC by markers (CD105 and CD90 by Flow cytometry) and proliferation rate *in vitro*. Single-color controls were acquired to make a compensation matrix for each test, and the signal visually gauged when gating for positive cells. **C.** CellTrace™ Far Red-labeled MSCs (white arrow) were detected only in stenotic kidneys injected with MSC (top, x10 images), but not in negative control untreated with MSCs. Cytokeratin (green) was stained as reference for tubular cells.

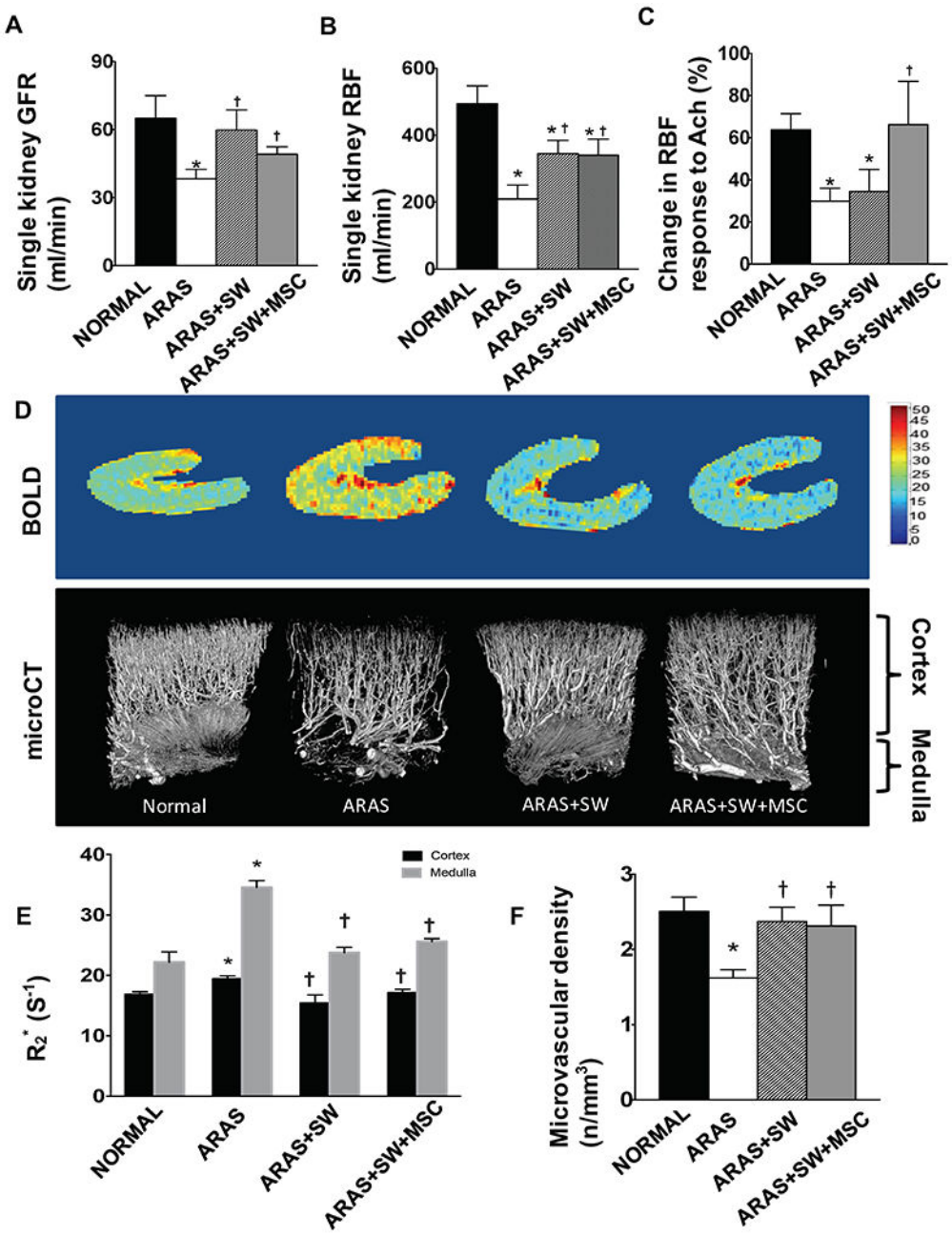

Figure 2.

A-C: Single-kidney glomerular filtration rate (GFR) and renal blood flow (RBF) in pigs with atherosclerotic renal artery stenosis (ARAS), untreated or treated with a shockwave (SW) regimen with or without an intra-renal delivery of adipose tissue-derived mesenchymal stem/stromal cells (MSCs). RBF and GFR of the stenotic ARAS kidney decreased compared to normal, but increased by both SW and SW+MSC to a similar extent. Compared to Normal, the ARAS and ARAS+SW groups had blunted RBF responses to acetylcholine (Ach), which was normalized in the ARAS+SW+MSC group. D: Representative images of blood-oxygen-level-dependent magnetic resonance imaging and micro-computed tomography, and quantification of microvascular density and hypoxia (R2*). E: Cortical and medullary

oxygenation was decreased in ARAS compared to Normal, and both were improved by SW and SW+MSC. F: Both SW and SW+MSC improved cortical vascular density that was decreased in ARAS. *p<0.05 vs. Normal, † p<0.05 vs. ARAS (n=5-6/group). Results are mean±SEM.

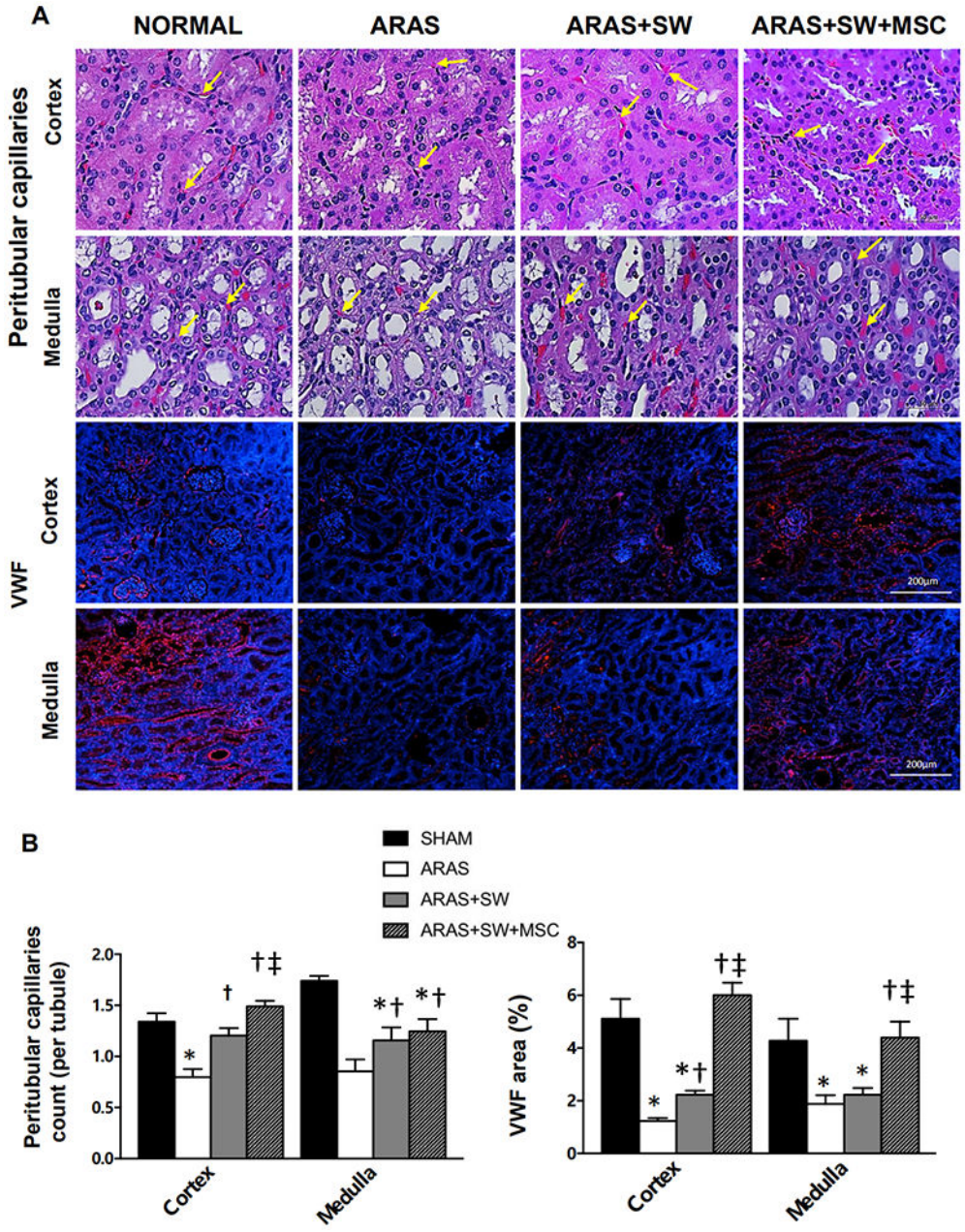

Figure 3.

A: Representative H&E-stained cortical and medullary sections (x40 images) and immunofluorescent staining of von Willebrand factor (vWF) (x10, positive staining red, nuclei blue). Capillaries (yellow arrow) were identified by the presence of lumen, red blood cells, and/or endothelial cell lining. B: The number of capillaries-per-tubule decreased in ARAS compared to Normal (H&E, performed at x100), but increased after SW and SW +MSC in ARAS. Cortical capillary density in ARAS+SW+MSC was higher than in ARAS +SW. vWF expression in cortex and medulla was diminished in ARAS and ARAS+SW, but restored to normal in ARAS+SW+MSC. *p<0.05 vs. Normal, †p<0.05 vs. ARAS, ‡p<0.05 vs. ARAS+SW (n=5-6/group). Results are mean±SEM.

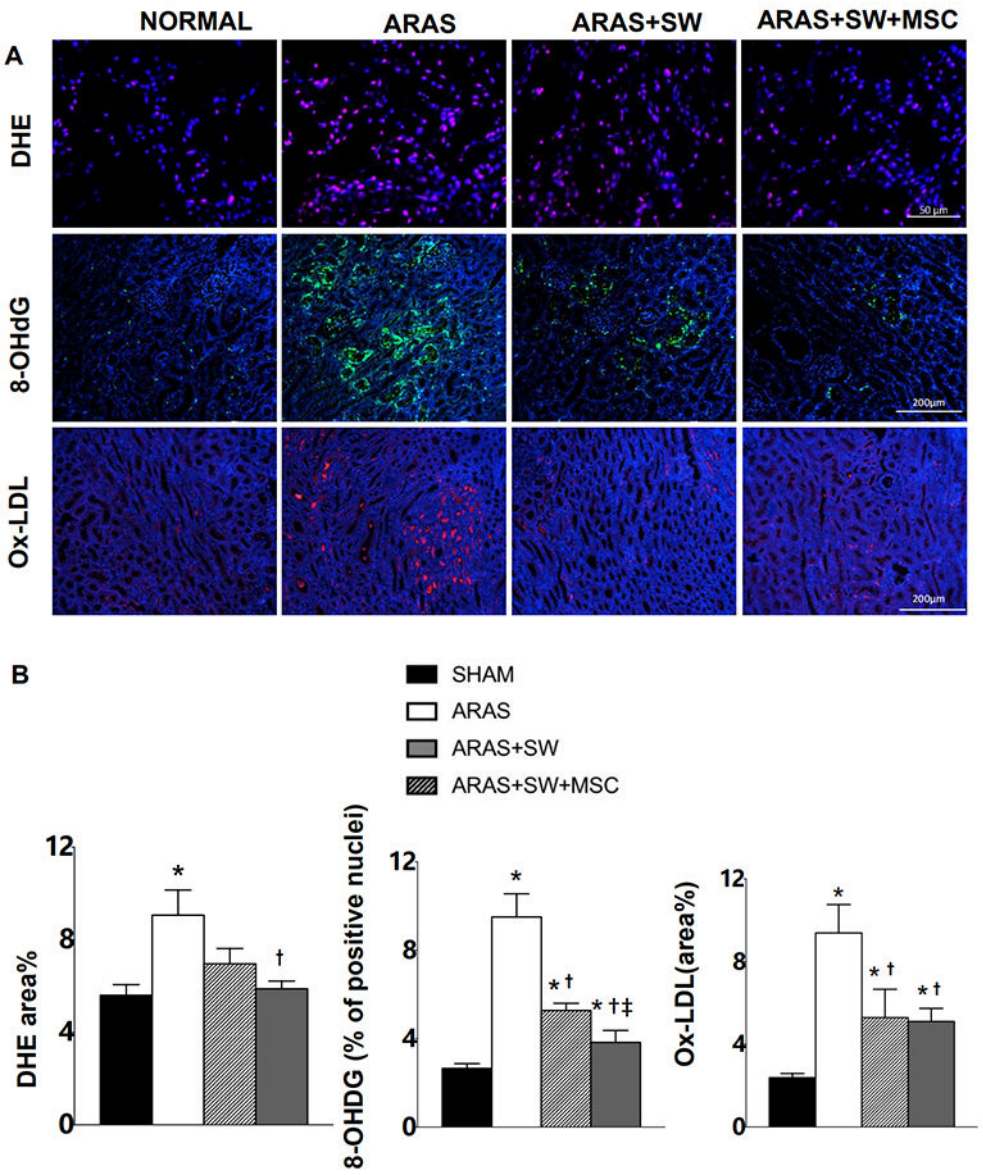

Figure 4.

A: Representative images of dihydroethidium (DHE) (40×, positive staining pink, nuclei blue], immunofluorescence staining for expression of 8-hydroxy-2' -deoxyguanosine (8-OHdG) (10×, green, nuclei blue) and oxidized low density lipoprotein (Ox-LDL) (10×, red, nuclei blue). B: Renal oxidative stress evaluated by DHE in ARAS+SW was not different from ARAS, whereas SW+MSC decreased renal oxidative stress in ARAS. Increased expression of 8-OHdG in ARAS was attenuated by SW, and further by SW+MSC. SW and SW+MSC similarly decreased elevated expression of Ox-LDL in ARAS. *p<0.05 vs. Normal, † p<0.05 vs. ARAS (n=5-6/group). *p<0.05 vs. Normal, † p<0.05 vs. ARAS, ‡p<0.05 vs. ARAS+SW (n=5/6). Results are mean±SEM.

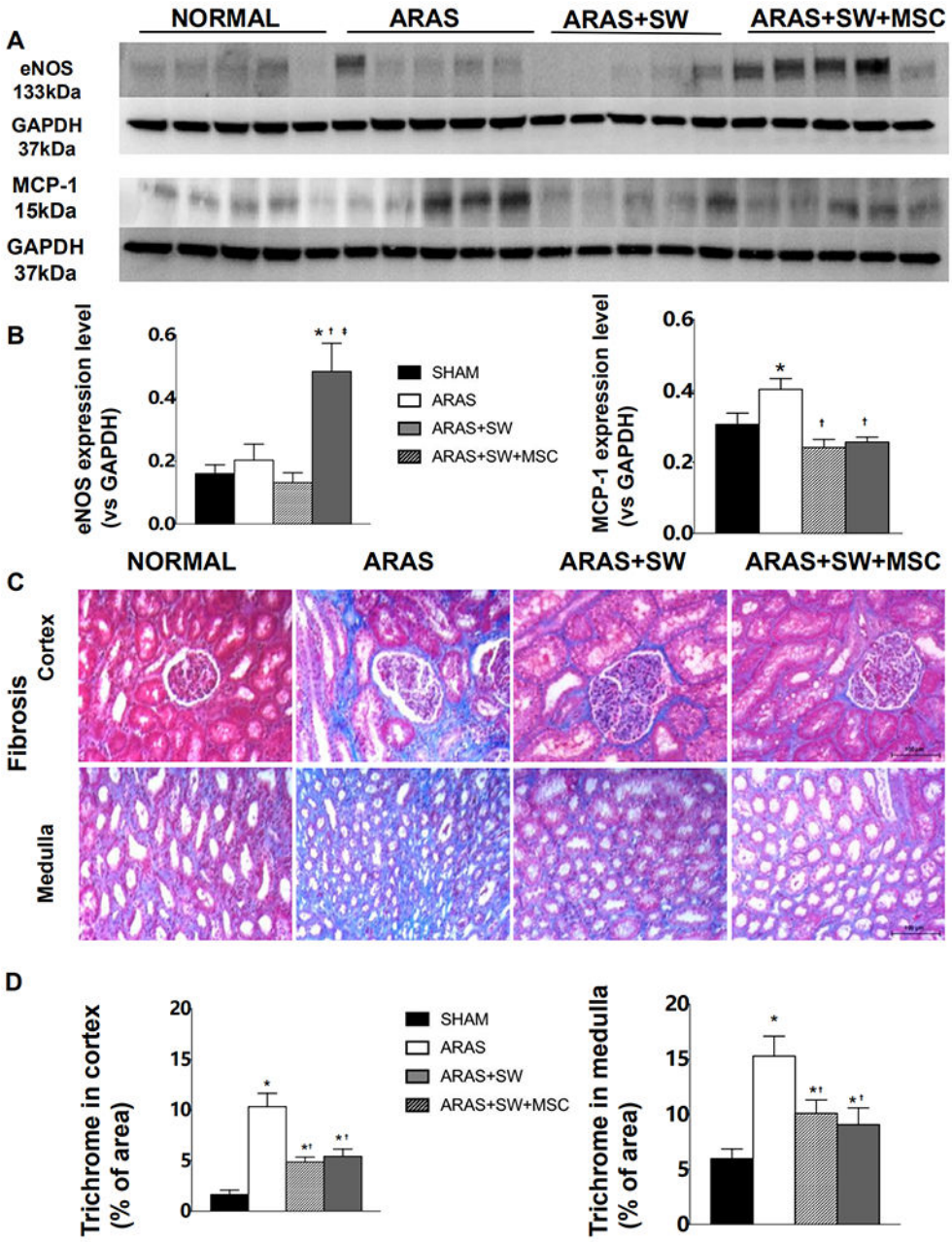

Figure 5.

A: Renal expression of endothelial nitric oxide synthase (eNOS) and monocyte chemoattractant protein (MCP)-1. B: Expression of eNOS increased in ARAS+SW+MSC compared to all other groups; MCP-1 expression increased in ARAS and was normalized by all treatments. C: Representative trichrome-stained cortex and medulla (x20). D: ARAS increased trichrome staining compared to Normal, which was alleviated both by SW and SW +MSC. *p<0.05 vs. Normal, †p<0.05 vs. ARAS, ‡p<0.05 vs. ARAS+SW(n=5-6/group). Results are mean±SEM.

Table 1.

Characteristics of pigs with atherosclerotic renal artery stenosis (ARAS), 4 weeks after treatment with mesenchymal stem/stromal cells (MSCs) without or with a preceding shockwave (SW) regimen.

Characteristics	Normal (n=6)	ARAS (n=6)	ARAS+SW (n=5)	ARAS+SW+MSC (n=5)
Body Weight (kg)	51.9±2.6	48.4±5.8	56.6±4.2	56.4±2.6
Degree of stenosis (%)	0	86±3.5	81±9.3	83±11.2
MAP (mmHg)	98±5	132±11 *	120±9 *	127±13 *
PRA (renal vein, pg/ml)	0.13±0.08	5.66±3.40 *	0.51±0.27 *†	0.58±0.38 *†
TNF-a (renal vein, pg/ml)	27.66±4.09	112.99±54.94 *	41.47±4.79 *‡	48.88±4.98 *‡
IL-10 (renal vein, pg/ml)	18.40±7.50	16.73±3.87	55.92±34.27 #‡	67.04±22.45 *†
IF-γ (renal vein, pg/ml)	0.055(0.024-0.26)	0.061(0.038-0.44)	0.23(0.018-0.76)	0.173(0-0.73)

MAP, mean arterial pressure; PRA, plasma renin activity; TNF-a, tumor necrosis factor–α; IL-10, interleukin-10; IF-γ, interferon-γ.

* p<0.05 vs. Normal

† p<0.05 vs. ARAS

p=0.1 vs. Normal

‡ p=0.1 vs. ARAS